Downloaded from rsta.royalsocietypublishing.org

PHILOSOPHICAL TRANSACTIONS OF THE ROYAL SOCIETY A MATHEMATICAL, PHYSICAL & ENGINEERING SCIENCES

# Riemann Problems and the WAF Method for Solving the Two-Dimensional Shallow Water Equations

E. F. Toro

*Phil. Trans. R. Soc. Lond. A* 1992 **338**, 43-68
doi: 10.1098/rsta.1992.0002

**Email alerting service** Receive free email alerts when new articles cite this article - sign up in the box at the top right-hand corner of the article or click **here**

To subscribe to *Phil. Trans. R. Soc. Lond. A* go to:
**http://rsta.royalsocietypublishing.org/subscriptions**

This journal is © 1992 The Royal Society

Downloaded from rsta.royalsocietypublishing.org

MATHEMATICAL, PHYSICAL & ENGINEERING SCIENCES
THE ROYAL SOCIETY A
PHILOSOPHICAL TRANSACTIONS OF

# Riemann problems and the WAF method for solving the two-dimensional shallow water equations

By E. F. Toro

*Department of Aerodynamics and Fluid Mechanics, College of Aeronautics, Cranfield Institute of Technology, Cranfield, Bedford MK43 0AL, U.K.*

## Contents

1. Introduction 43
2. The Riemann problem 45
   (*a*) An exact Riemann solver 46
   (*b*) Solution to the Riemann problem 48
   (*c*) Approximate Riemann solvers 51
3. The weighted average flux method (WAF) 56
   (*a*) Formulations of the method 56
   (*b*) Sonic flow 57
   (*c*) A TVD version of the WAF method 58
   (*d*) The CFL condition 59
   (*e*) Boundary conditions 60
   (*f*) Extensions of the WAF method 60
   (*g*) An algorithm for the one-dimensional case 62
4. Test problems 62
5. Conclusions 66
   References 67

An exact Riemann solver for the shallow water equations along with several approximate Riemann solvers are presented. These solutions are then used locally to help compute numerically the global solution of the general initial boundary value problem for the shallow water equations. The numerical method used is the weighted average flux method (WAF) proposed by the author. This is a conservative, shock capturing high resolution TVD method. For shallow water flows where nonlinear effects are important or where abrupt changes (hydraulic jumps) are to be expected the present algorithms can be useful in practice. One and two-dimensional solutions are presented to assess both the Riemann solvers and the WAF method.

## 1. Introduction

A wide variety of physical phenomena are governed by the shallow water equations. Some examples are tides in oceans, breaking of waves in shallow beaches, open-channel flow problems such as roll waves, flood waves in rivers and surges. Also, the equations can be reinterpreted and used to model flows in the atmosphere.

The shallow water equations are a set of nonlinear hyperbolic equations and are an approximation to the full free-surface gravity flow problem with viscosity and surface tension effects neglected. The key assumption contained in the shallow-water

*Phil. Trans. R. Soc. Lond.* A (1992) **338**, 43–68
*Printed in Great Britain*



The Royal Society is collaborating with JSTOR to digitize, preserve, and extend access to *Philosophical Transactions: Physical Sciences and Engineering.* www.jstor.org

Downloaded from rsta.royalsocietypublishing.org



equations is that the vertical component of the acceleration of the water particles has a negligible effect on the pressure, or equivalently that the pressure is given as in hydrostatics. The same governing equations result as the approximation of lowest order in a perturbation procedure. This involves a formal development of all quantities in powers of a parameter, $\epsilon$, which is the ratio of the water depth to some other characteristic length associated with the horizontal direction.

The second approach to deriving the shallow water equations makes evident the role played by the undisturbed water depth in determining the accuracy of the approximation. More details can be found in Stoker (1957).

The nonlinear character of the equations means that the use of analytical techniques to solve them can only be successful in very special circumstances. Numerical methods must be used to obtain solutions to realistic problems of scientific or engineering interest. But it is the hyperbolic character of the shallow water equations that makes the mathematical and numerical problems of finding solutions difficult.

Hyperbolic equations admit discontinuous solutions, in addition to smooth or classical solutions. Even for the case in which the initial data is smooth everywhere, the nonlinear character combined with the hyperbolic type of the equations can lead to discontinuous solutions in a finite time. In the field of gas dynamics, the discontinuities are associated with shock waves and contact surfaces. In the context of the shallow water equations the discontinuities are associated with hydraulic jumps and bores in water or the propagation of sharp fronts in the atmosphere.

For a large variety of flow situations one may assume that solutions remain smooth for all times. The development and application of numerical methods for the shallow water equations in these circumstances form an impressive body of research work. An up-to-date survey in this area is contained in the paper by Casulli (1990).

In this paper we are concerned with numerical methods for simulating flow situations in which discontinuities are present and are important to model. In particular, we describe the application of the weighted average flux (WAF) method to the two-dimensional shallow water equations. This is a shock-capturing, high-resolution conservative method that is based on solutions to local Riemann problems. The WAF approach was presented by the author (Toro 1989*a*), as applied to systems of nonlinear hyperbolic conservation laws. Applications of the method to problems related to gas dynamics with shock waves have been very successful (Toro 1989*a*, 1990). We can now use the resulting experience to exploit the specific features of the shallow water equations to formulate simple and robust numerical procedures based on the WAF principle.

The two-dimensional shallow water equations written in conservation form with source terms are

$$U_t + F_x + G_z = S(U) \tag{1}$$

with
$$U = \begin{bmatrix} \phi \\ \phi u \\ \phi w \end{bmatrix}, \quad F = \begin{bmatrix} \phi u \\ \phi u^2 + \frac{1}{2}\phi^2 \\ \phi uw \end{bmatrix}, \quad G = \begin{bmatrix} \phi w \\ \phi uw \\ \phi w^2 + \frac{1}{2}\phi^2 \end{bmatrix}, \quad S = \begin{bmatrix} 0 \\ g\phi h_x \\ g\phi h_z \end{bmatrix}. \tag{2}$$

In equation (1) $U$ is the vector of 'conserved' variables, $F(U)$ and $G(U)$ are flux vectors, $S(U)$ is a 'source' term vector. Figure 1 illustrates the flow configuration that gives rise to the model (1)–(2). Details on the derivation of the equations can be found in Stoker (1957) and Glaister (1987). Here $g$ is the acceleration due to gravity, $h+\eta$

Downloaded from rsta.royalsocietypublishing.org



is the total depth, $\phi = g(h+\eta)$, $u$ and $w$ are the $x$ and $z$ components of velocity respectively.

For many applications there will be additional terms in the vector $S(U)$ to account for Coriolis force and bottom friction. The numerical solution procedure described in §§2–4 deals essentially with the homogeneous part of equation (1). The treatment of the source terms is a relatively standard process via time operator splitting. Moreover, the two-dimensional homogeneous problem is solved by using space splitting, or method of fractional steps, whereby the two-dimensional problem is reduced to a sequence of one-dimensional problems. Splitting procedures are presented in §4. It is therefore sufficient to consider

$$U_t + F_x = 0. \tag{3}$$

This homogeneous conservation law can be rewritten in integral form as

$$\oint (U\,\mathrm{d}x - F\,\mathrm{d}t) = 0, \tag{4}$$

which is more general than (3), for it admits discontinuous solutions.

This paper is organized as follows. In §2 we formulate the Riemann problem, present an exact solver and a variety of approximate solution procedures. In §3 we present the WAF numerical method and its practical implementation for the shallow water equations. In §4 we apply the method to test problems in one and two dimensions. Conclusions are drawn in §5.

## 2. The Riemann problem

The numerical technique WAF described in this paper uses solutions to local Riemann problems to evolve the global solution in time. For simplicity we consider first the Riemann problem for the purely one-dimensional case,

$$\begin{bmatrix} \phi \\ \phi u \end{bmatrix}_t + \begin{bmatrix} \phi u \\ \phi u^2 + \frac{1}{2}\phi^2 \end{bmatrix}_x = 0, \quad t > 0, \quad -\infty < x < \infty. \tag{5}$$

The Riemann problem for (5) is the initial value problem (IVP) for (5) with piecewise constant initial data.

$$U(0,x) = \begin{cases} U_{\mathrm{L}}, & x < 0, \\ U_{\mathrm{R}}, & x > 0. \end{cases} \tag{6}$$

The subscripts L and R denote left and right states respectively.

It is easy to see that the system (5) is hyperbolic with real eigenvalues

$$e_1 = u - a, \quad e_2 = u + a, \tag{7}$$

where

$$a = \sqrt{\phi} = \sqrt{[g(\eta + h)]} \tag{8}$$

denotes the 'sound' speed, or celerity.

The IVP (5)–(6) can be solved exactly. This is possible because of the simplicity of the initial condition (6). The solution can be represented in the $xt$-plane as shown in figure 2. There are two waves, one travels to the left and the other to the right. They can either be shock (bore) or rarefaction (depression) waves. Figure 3 shows all four

Downloaded from rsta.royalsocietypublishing.org



Figure 1

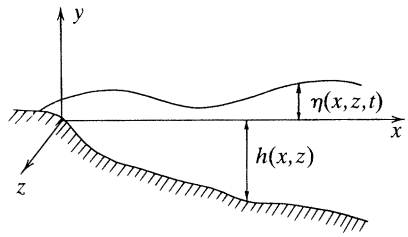


Figure 2

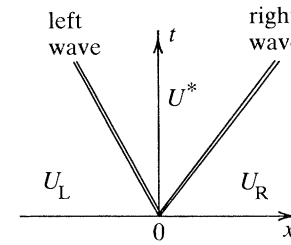


Figure 1. Free-surface flow configuration. $(x, z)$ is horizontal plane, $y$ is vertical direction, $h(x, z)$ is depth of undisturbed water, $\eta(x, z, t)$ is free surface disturbance.

Figure 2. Wave pattern of solution of the Riemann problem for the one-dimensional shallow-water equations.

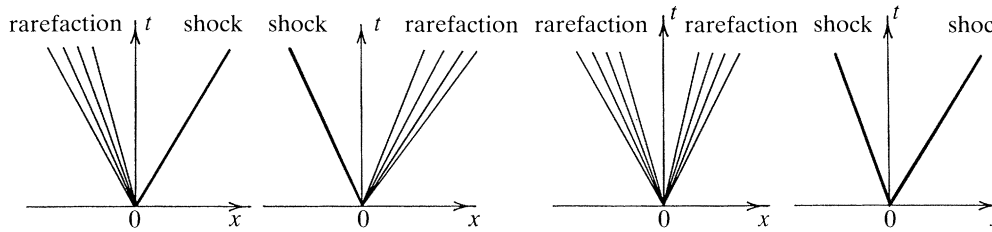


Figure 3. All possible wave configurations in the solution of the Riemann problem for the one-dimensional shallow-water equations.

possible wave patterns. The waves separate three constant states, namely $U_L$ (data) to the left of the left wave, $U_R$ (data) to the right of the right wave and a new constant state $U^*$ valid in the region between the left and right waves. We denote this region by the *star region*. The solution through rarefaction waves, at any given time $t^*$, varies continuously with $x$, while through shock waves it jumps discontinuously.

### (a) *An exact Riemann solver*

The main step in solving the Riemann problem is to find the constant state $U^*$ in the star region (see figure 2). This depends on appropriate relations through the left and right waves connecting $U^*$ to the data states $U_L$ and $U_R$ respectively. Such relations depend on the type of waves present, but this is not known *a priori*. It could be any of the four patterns shown in figure 3. The determination of the wave type is part of the solution procedure, which is iterative.

Marshall & Mendez (1981) appear to be the first to have solved the Riemann problem for the shallow water exactly. Their method is based on the Godunov's iteration procedure, which is known to be very inefficient due to its low rate of convergence.

The exact Riemann solver to be described next follows the ideas behind the Riemann solver for covolume gases presented in Toro (1989*c*). Essentially, we derive a single (nonlinear) algebraic equation for $\phi^*$, the value of $\phi$ in the star region, namely

$$f(\phi^*) \equiv f_L(\phi^*, \phi_L) + f_R(\phi^*, \phi_R) + u_R - u_L = 0. \tag{9}$$

Our solution procedure is, computationally, very efficient. Here $u_L$ and $u_R$ are velocity on left and right states respectively (data); $f_L$ and $f_R$ are functions

Downloaded from rsta.royalsocietypublishing.org



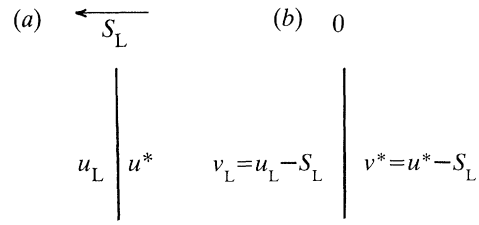


Figure 4. Transformation to a steady frame of reference moving with the shock speed.

connecting the left and right states respectively, to the star region. In what follows we shall derive expressions for the functions $f_L$ and $f_R$. As already mentioned, they depend on the type of waves present. We consider each case separately.

(i) *A left shock wave*

Here we suppose that the left wave is a shock wave travelling with velocity $S_L$. It is convenient to transform coordinates to a stationary frame as shown in figure 4, where

$$v_L = u_L - S_L, \quad v^* = u^* - S_L. \tag{10}$$

In this frame the conservation laws (5) give

$$\phi_L v_L = \phi^* v^* \equiv M_L, \tag{11}$$

$$\phi_L v_L^2 + \tfrac{1}{2}\phi_L^2 = \phi^* v^{*2} + \tfrac{1}{2}\phi^{*2}. \tag{12}$$

The convenience of transforming to a stationary frame is that the jump conditions are easier to apply, without having to solve for $S_L$ explicitly, which in any case is not needed, in solving for $\phi^*$.

Equation (12) can be rewritten as

$$(\phi_L v_L) v_L - (\phi^* v^*) v^* = \tfrac{1}{2}(\phi^{*2} - \phi_L^2),$$

which after inserting $M_L$ from (11) gives

$$M_L = -\tfrac{1}{2}(\phi^{*2} - \phi_L^2)/(v^* - v_L) = -\tfrac{1}{2}(\phi^{*2} - \phi_L^2)/(u^* - u_L). \tag{13}$$

From equation (11) again we have $v^* = M_L/\phi^*$ and $v_L = M_L/\phi_L$ and so (13), after some manipulations, becomes

$$M_L = [\tfrac{1}{2}\phi_L \phi^*(\phi_L + \phi^*)]^{\frac{1}{2}}. \tag{14}$$

From equation (13) we obtain

$$u^* = u_L - \tfrac{1}{2}(\phi^{*2} - \phi_L^2)/M_L,$$

or

$$u^* = u_L - f_L(\phi^*, \phi_L), \tag{15}$$

where

$$f_L(\phi^*, \phi_L) = (\phi^* - \phi_L)\,[\tfrac{1}{2}(\phi^* + \phi_L)/\phi^*\phi_L]^{\frac{1}{2}}. \tag{16}$$

We have obtained the function $f_L$ for the case in which the left wave is a shock wave.

(ii) *A right shock wave*

We proceed in an analogous way as in the case of a left shock. Suppose the right shock travels with speed $S_R$. In the stationary frame of reference we define

$$v^* = u^* - S_R, \quad v_R = u_R - S_R \tag{17}$$

Downloaded from rsta.royalsocietypublishing.org



so that the conservation equations (5) become

$$\phi^* v^* = \phi_R v_R \equiv -M_R, \tag{18}$$

$$\phi^* v^{*2} + \tfrac{1}{2}\phi^{*2} = \phi_R v_R^2 + \tfrac{1}{2}\phi_R^2. \tag{19}$$

Equations (17)–(19) give

$$M_R = \tfrac{1}{2}(\phi^{*2} - \phi_R^2)/(u^* - u_R) = \tfrac{1}{2}(\phi^{*2} - \phi_R^2)/(v^* - v_R), \tag{20}$$

or

$$M_R = [\tfrac{1}{2}\phi^* \phi_R(\phi^* + \phi_R)]^{\frac{1}{2}}. \tag{21}$$

From equation (20) we obtain

$$u^* = u_R + \tfrac{1}{2}(\phi^{*2} - \phi_R^2)/M_R,$$

or

$$u^* = u_R + f_R(\phi^*, \phi_R), \tag{22}$$

where

$$f_R(\phi^*, \phi_R) = (\phi^* - \phi_R)\,[\tfrac{1}{2}(\phi^* + \phi_R)/(\phi^* \phi_R)]^{\frac{1}{2}}. \tag{23}$$

This is the function $f_R$ for the case of a right shock wave. Note that by subtracting (15) from (22) $u^*$ is eliminated leaving a single algebraic equation of the form (9) for the unknown $\phi^*$.

(iii) *Rarefaction waves*

The case of rarefaction waves is most easily dealt with by rewriting equations (5) in non-conservative form and noting that the Riemann invariants (Stoker 1957) are

$$u - 2a = I_L \quad \text{along curves} \quad \mathrm{d}x/\mathrm{d}t = u - a, \tag{24}$$

$$u + 2a = I_R \quad \text{along curves} \quad \mathrm{d}x/\mathrm{d}t = u + a, \tag{25}$$

where $I_L$ and $I_R$ are constant.

If the left wave is a rarefaction wave we can connect the left state $U_L$ to the unknown state $U^*$ across the left wave by transversing it with a wave of the family $\mathrm{d}x/\mathrm{d}t = u + a$, along which the right Riemann invariant $I_R$ in (25) is constant, i.e.

$$u_L + 2a_L = u^* + 2a^*.$$

Hence

$$u^* = u_L - f_L(\phi^*, \phi_L), \tag{26}$$

$$f_L = 2(\sqrt{\phi^*} - \sqrt{\phi_L}). \tag{27}$$

Similarly for a right rarefaction wave we have

$$u^* = u_R + f_R(\phi^*, \phi_R) \tag{28}$$

with

$$f_R = 2(\sqrt{\phi^*} - \sqrt{\phi_R}). \tag{29}$$

The equation (9) for the unknown $\phi^*$ is now completely determined.

### (b) *Solution to the Riemann problem*

For convenience we summarize the expressions for $f_L$ and $f_R$, namely

$$f_L = \begin{cases} 2(\sqrt{\phi^*} - \sqrt{\phi_L}), & \text{left rarefaction}, \quad \phi^* \leqslant \phi_L, \\ (\phi^* - \phi_L)\sqrt{[\tfrac{1}{2}(\phi^* + \phi_L)/(\phi^* \phi_L)]}, & \text{left shock}, \quad \phi^* > \phi_L, \end{cases} \tag{30}$$

$$f_R = \begin{cases} 2(\sqrt{\phi^*} - \sqrt{\phi_R}), & \text{right rarefaction}, \quad \phi^* \leqslant \phi_R, \\ (\phi^* - \phi_R)\sqrt{[\tfrac{1}{2}(\phi^* + \phi_R)/(\phi^* \phi_R)]}, & \text{right shock}, \quad \phi^* > \phi_R. \end{cases} \tag{31}$$

Downloaded from rsta.royalsocietypublishing.org



The choice of the particular form of $f_L, f_R$ depends physically on the ratios $\phi^*/\phi_L$, $\phi^*/\phi_R$. It can be shown that $f(\phi)$ as given by (9) with $f_L$ and $f_R$ chosen as in (30), (31) is a monotone function and has therefore a unique solution for physically admissible data.

The nonlinear equation (9) can thus be solved using a Newton–Raphson iteration procedure

$$\phi^*_{(k)} = \phi^*_{(k-1)} + \sigma_{(k-1)}, \tag{32}$$

where

$$\sigma_{(k)} = -f_{(k)}/f'_{(k)}, \tag{33}$$

with $k$ denoting the iteration number, and $f' \equiv \mathrm{d}f/\mathrm{d}\phi^* = f'_L + f'_R$ denoting the first derivative of $f$ with respect to $\phi^*$. From (30)–(31) $f'_L$ and $f'_R$ are found to be

$$f'_L = \begin{cases} 1/\sqrt{\phi^*}, & \text{left rarefaction,} \\ D_L - \frac{1}{4}(\phi^* - \phi_L)/D_L\,\phi^{*2}, & \text{left shock,} \end{cases} \tag{34}$$

$$f'_R = \begin{cases} 1/\sqrt{\phi^*}, & \text{right rarefaction,} \\ D_R - \frac{1}{4}(\phi^* - \phi_R)/D_R\,\phi^{*2}, & \text{right shock,} \end{cases} \tag{35}$$

where

$$D_L = \sqrt{[\tfrac{1}{2}(\phi^* + \phi_L)/(\phi^*\phi_L)]}, \quad D_R = \sqrt{[\tfrac{1}{2}(\phi^* + \phi_R)/(\phi^*\phi_R)]}. \tag{36}$$

The iteration (32) requires an initial guess $\phi^*_{(0)}$ for $\phi^*$. One could take $\phi_{(0)} = \frac{1}{2}(\phi_L + \phi_R)$ for instance, which although simple is not very accurate. The initial guess

$$\phi^*_{(0)} = [\tfrac{1}{2}(\sqrt{\phi_L} + \sqrt{\phi_R}) + \tfrac{1}{4}(u_L - u_R)]^2 \tag{37}$$

is found to be very accurate for most pairs of states $(U_L, U_R)$ in a typical flow field. However, it is costly to compute, but for some tests we have carried out there are net gains in using it.

The iteration procedure is stopped whenever

$$\sigma = |\phi^*_{(k)} - \phi^*_{(k-1)}|/\phi^*_{(k)} \leqslant \tau,$$

where $\tau$ is a chosen tolerance. For most purposes $\tau = 10^{-4}$ is good enough. Once $\phi^*$ is known, $u^*$ can be computed from (26) or (28) or a combination of the two as

$$u^* = \tfrac{1}{2}(u_R + u_L) + \tfrac{1}{2}(f_R - f_L). \tag{38}$$

(i) *Shock wave speeds*

The speed $S_L$ for a left shock can be calculated once $\phi^*$ is known. From equation (11) we have $\phi_L v_L = M_L$, where $M_L$, given by equation (14), is now known. From equation (10) $v_L = u_L - S_L$ and so $\phi_L(u_L - S_L) = M_L$, from which the speed $S_L$ follows as

$$S_L = u_L - M_L/\phi_L. \tag{39}$$

Similar arguments give the speed $S_R$ for a right shock as

$$S_R = u_R + M_R/\phi_R. \tag{40}$$

(ii) *Solution inside rarefaction fans*

Suppose the left wave is a rarefaction wave (see figure 5). The head of the fan is given by the ray $\mathrm{d}x/\mathrm{d}t = u_L - a_L$ and the tail is given by the ray $\mathrm{d}x/\mathrm{d}t = u^* - a^*$. Suppose we wish to find the solution inside the fan at the point $(\hat{x}, \hat{t})$ say. Denote by

Downloaded from rsta.royalsocietypublishing.org



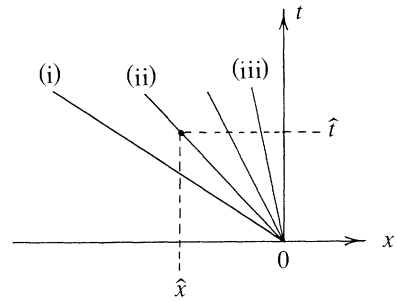


Figure 5. Determination of the solution inside a rarefaction fan. (i) $\mathrm{d}x/\mathrm{d}t = u_{\mathrm{L}} - a_{\mathrm{L}}$; (ii) $\mathrm{d}x/\mathrm{d}t = \hat{x}/\hat{t}$; (iii) $\mathrm{d}x/\mathrm{d}t = u^* - a^*$.

$u$ and $a$ the unknown values for the particle speed and the celerity. Consider the ray passing through $(0,0)$ and $(\hat{x},\hat{t})$ for which $\mathrm{d}x/\mathrm{d}t = u - a$. Then

$$\hat{x}/\hat{t} = u - a. \tag{41}$$

Also, using the right Riemann invariant (25) across the left rarefaction we obtain

$$u + 2a = u_{\mathrm{L}} + 2a_{\mathrm{L}} \tag{42}$$

the solution of (41)–(42) for $u$ and $a$ is

$$u = \tfrac{1}{3}(u_{\mathrm{L}} + 2a_{\mathrm{L}} + 2\hat{x}/\hat{t}), \tag{43}$$

$$a = \tfrac{1}{3}(u_{\mathrm{L}} + 2a_{\mathrm{L}} - \hat{x}/\hat{t}). \tag{44}$$

For the case of a right rarefaction the head is given by $\mathrm{d}x/\mathrm{d}t = u_{\mathrm{R}} + a_{\mathrm{R}}$ and the tail by $\mathrm{d}x/\mathrm{d}t = u^* + a^*$. The solution at a point $(\hat{x},\hat{t})$ inside the fan is found to be

$$u = \tfrac{1}{3}(u_{\mathrm{R}} - 2a_{\mathrm{R}} + 2\hat{x}/\hat{t}), \tag{45}$$

$$a = \tfrac{1}{3}(-u_{\mathrm{R}} + 2a_{\mathrm{R}} + \hat{x}/\hat{t}). \tag{46}$$

The exact solution of the Riemann problem for the one-dimensional shallow water equations (5) is now complete.

(iii) *The Riemann problem for the split two-dimensional case*

When extending the WAF method to two space dimensions one considers the associated Riemann problem for the equations in one direction only, say $x$. Then the equations to consider are

$$\begin{bmatrix} \phi \\ \phi u \\ \phi w_t \end{bmatrix} + \begin{bmatrix} \phi u \\ \phi u^2 + \frac{1}{2}\phi_x^2 \\ \phi u w \end{bmatrix} = 0. \tag{47}$$

This system is hyperbolic and has three distinct eigenvalues

$$e_1 = u - a, \quad e_2 = u, \quad e_3 = u + a. \tag{48}$$

It is not difficult to see that the third equation involving the $z$-component of velocity $w$ is decoupled from the previous two equations; $w$ is passively advected by the speed $u$. The variables $u$ and $\phi$ are constant (as in one-dimensional case) in the star region between the acoustic waves $e_1 = u - a$ and $e_3 = u + a$, while $w$ only

Downloaded from rsta.royalsocietypublishing.org



changes (discontinuously) across $\mathrm{d}x/\mathrm{d}t = e_2 = u$, which is a linearly degenerate field. So the exact solution of the Riemann problem for (47) with data $(\phi_{\mathrm{L}}, u_{\mathrm{L}}, w_{\mathrm{L}})$ and $(\phi_{\mathrm{R}}, u_{\mathrm{R}}, w_{\mathrm{R}})$ is exactly the same as in the one-dimensional case, for the unknowns $\phi^*$ and $u^*$, with the addition

$$w(x,t) = \begin{cases} w_{\mathrm{L}}, & \text{if} \quad x/t < u^*, \\ w_{\mathrm{R}}, & \text{otherwise.} \end{cases} \tag{49}$$

This particularly simple structure of the solution of the Riemann problem associated with the two-dimensional shallow water equations will be exploited when searching for approximations.

### (c) *Approximate Riemann solvers*

Although the exact Riemann solver presented in the previous section is very efficient, the search for approximate Riemann solvers is still justified. One would like to have to perform fewer and simpler operations. Perhaps more importantly, it is desirable to eliminate altogether the iteration procedure contained in the exact solver. This can result in significant additional computing savings in vector machines. The great advantage of using exact solvers is the added robustness of the codes under severe conditions. In the field of gas dynamics all the approximate Riemann solvers known to the author have limitations under certain circumstances. For the shallow water equations, however, it appears as if certain approximations can be very robust and simple to compute.

We present several approximate Riemann solvers.

#### (i) *A two rarefaction approximate solver* (TR)

This approximation results from assuming *a priori* that the two 'acoustic' waves present in the solution of the Riemann problem are both rarefaction waves (see figures 2 and 3). Of course this assumption may not be true, but it is remarkable the resulting approximate solution is quite accurate (Osher & Solomon 1982). An immediate consequence is that the functions $f_{\mathrm{L}}$ and $f_{\mathrm{R}}$ in equation (9) are those corresponding to rarefaction waves. Thus $f(\phi^*)$ in equation (9) becomes

$$2(\sqrt{\phi^*} - \sqrt{\phi_{\mathrm{L}}}) + 2(\sqrt{\phi^*} - \sqrt{\phi_{\mathrm{R}}}) + u_{\mathrm{R}} - u_{\mathrm{L}} = 0$$

from which the solution for $\phi^*$ follows directly as

$$\phi^* = [\tfrac{1}{2}(\sqrt{\phi_{\mathrm{L}}} + \sqrt{\phi_{\mathrm{R}}}) - \tfrac{1}{4}(u_{\mathrm{R}} - u_{\mathrm{L}})]^2. \tag{50}$$

The solution for $u^*$ follows from (38), as

$$u^* = \tfrac{1}{2}(u_{\mathrm{L}} + u_{\mathrm{R}}) + \sqrt{\phi_{\mathrm{L}}} - \sqrt{\phi_{\mathrm{R}}}. \tag{51}$$

For the case of the split two-dimensional Riemann problem for equations (47) one only needs to add the solution for $w$ as given by equation (49).

The TR approximation is exact for the case of two rarefaction waves in the Riemann problem, as well as for combinations of rarefactions and 'Mach' waves (waves of zero strength). It is also found to be quite accurate even for cases involving shock waves, as it will be seen later. More importantly, for a typical, one-dimensional calculation say, we may have to solve 100 Riemann problems at each time step. The most likely event is that only a couple of those Riemann problems may contain shock waves. The rest of the flow field can be accurately modelled by the two-rarefaction approximation.



PHILOSOPHICAL TRANSACTIONS OF THE ROYAL SOCIETY A MATHEMATICAL, PHYSICAL & ENGINEERING SCIENCES

PHILOSOPHICAL TRANSACTIONS OF THE ROYAL SOCIETY A MATHEMATICAL, PHYSICAL & ENGINEERING SCIENCES

Downloaded from rsta.royalsocietypublishing.org



(ii) *Choice of wave speeds*

The WAF method, to be described in §3, requires the wave speeds and the states separated by the waves. In the TR approximation the acoustic waves are assumed to be rarefactions and thus there is ambiguity when having to choose the representative wave speeds. We find that

$$\left.\begin{aligned} \lambda_1 &= \min\{u_L - a_L, \quad u^* - a^*\}, \\ \lambda_2 &= u^*, \\ \lambda_3 &= \max\{u_R + a_R, \quad u^* + a^*\}, \end{aligned}\right\} \tag{52}$$

is the best choice one can make from the information available in the TR approximation.

(ii) *The two-shock approximation* (TS)

This approximation results from assuming (which again may not be true) that the acoustic waves in the Riemann problem are both shock waves. The functions $f_L$ and $f_R$ in equation (9) are those corresponding to shocks in equations (30)–(31) and thus we obtain

$$(\phi^* - \phi_L)\sqrt{[\tfrac{1}{2}(\phi^* + \phi_L)/\phi^*\phi_L]} + (\phi^* - \phi_R)\sqrt{[\tfrac{1}{2}(\phi^* + \phi_R)/\phi^*\phi_R]} + u_R - u_L = 0. \tag{53}$$

Unfortunately, this is still a nonlinear equation for $\phi^*$ and I have not been able to find a closed-form solution for it. The advantage of using the TS approximation instead of the exact solver is that the computer logic associated with the type of waves is not present.

A possible further approximation to the TS approximation can be obtained by expanding (53) in a Taylor series about a point $\phi^*_{(0)}$ and retaining first-order terms. The point $\phi^*_{(0)}$ can be taken from the TS approximation (50). We find that we still need to solve a quadratic equation with coefficients involving many operations. We do not regard this approach as useful, although the solution for $\phi^*$ is then direct.

Once $\phi^*$ is obtained from the solution of (53) $u^*$ follows from equation (38) as

$$u^* = \tfrac{1}{2}(u_R + u_L) + \tfrac{1}{2}(f_R - f_L), \tag{54}$$

where, for consistency with the TS approximation, one takes $f_L$ and $f_R$ from the shock branches in (30)–(31).

The wave speeds $\lambda_1, \lambda_2, \lambda_3$ can be taken as those given by (52). Alternatively, one can test the ratios $\phi^*/\phi_L, \phi^*/\phi_R$. If either of these is greater than unity one could choose the exact shock-wave speeds $S_L$ or $S_R$, given by (39)–(40), for $\lambda_1$ or $\lambda_3$.

For the two-dimensional split case, again we choose $\lambda_2 = u^*$ and $w(x,t)$ as given by (49).

(iv) *Roe-type approximations*

Glaister (1987) derived a Roe-type approximation for the shallow water equations. There are two possible interpretations for this approximation. The first, is the original concept, due to Roe (1981). We denote this interpretation by RS1. This is the interpretation to be used in Roe's method. The second interpretation is new and can be used in the context of any Godunov-type methods, including WAF. We denote this approximation by RS2.

Downloaded from rsta.royalsocietypublishing.org



(v) *First interpretation of Roe's solver* (RS1)

For the purpose of using Roe's method one must obtain the Roe approximation to the solution of the Riemann problem. This makes use of the fact that for a linear hyperbolic system of the form (3) the flux difference $\Delta F = F_R - F_L$ between a left (L) and right (R) states can be written as

$$\Delta F = \sum_{k=1}^{N} \alpha_k \lambda_k r_k, \tag{55}$$

where $N$ is the number of waves in the Riemann problem with data $U_L$ and $U_R$, $\alpha_k$ are the wave strengths, $\lambda_k$ are the wave speeds or eigenvalues of the jacobian matrix $J = \partial F/\partial U$ and $r_k$ are the right eigenvectors corresponding to the eigenvalues $\lambda_k$. Note that (55) is in general a vector equation.

For linear systems with constant coefficients the jacobian matrix $J$ is constant. Roe's approximation is based on the assumption that the matrix $J$ is still constant for nonlinear systems. It is then a question of constructing appropriate averaged values $\tilde{U}$ in terms of the data states $U_L$ and $U_R$ such that $\tilde{J} = \tilde{J}(\tilde{U}) = \tilde{J}(U_L, U_R)$.

Glaister (1987) provided the Roe-averaged values for the two-dimensional shallow water equations. We simply state the result here.

$$\tilde{u} = (\sqrt{\phi_L}\, u_L + \sqrt{\phi_R}\, u_R)/(\sqrt{\phi_L} + \sqrt{\phi_R}), \tag{56a}$$

$$\tilde{w} = (\sqrt{\phi_L}\, w_L + \sqrt{\phi_R}\, w_R)/(\sqrt{\phi_L} + \sqrt{\phi_R}), \tag{56b}$$

$$\tilde{a} = \sqrt{\tfrac{1}{2}(\phi_L + \phi_R)}, \tag{56c}$$

$$\tilde{\phi} = \sqrt{(\phi_L \phi_R)}, \tag{56d}$$

$$\tilde{\lambda}_1 = \tilde{u} - \tilde{a}, \quad \tilde{\lambda}_2 = \tilde{u}, \quad \tilde{\lambda}_3 = \tilde{u} + \tilde{a}, \tag{56e}$$

$$\left.\begin{aligned} \tilde{\alpha}_1 &= \tfrac{1}{2}\Delta\phi - \tfrac{1}{2}\tilde{\phi}\Delta u/\tilde{a}, \\ \tilde{\alpha}_2 &= \tilde{\phi}\Delta w, \\ \tilde{\alpha}_3 &= \tfrac{1}{2}\Delta\phi + \tfrac{1}{2}\tilde{\phi}\Delta u/\tilde{a}, \end{aligned}\right\} \tag{56f}$$

where $\Delta\phi = \phi_R - \phi_L, \Delta u = u_R - u_L, \Delta w = w_R - w_L$.

The right eigenvectors are

$$\tilde{r}_1 = \begin{bmatrix} 1 \\ \tilde{u} - \tilde{a} \\ \tilde{w} \end{bmatrix}, \quad \tilde{r}_2 = \begin{bmatrix} 0 \\ 0 \\ 1 \end{bmatrix}, \quad \tilde{r}_3 = \begin{bmatrix} 1 \\ \tilde{u} + \tilde{a} \\ \tilde{w} \end{bmatrix}. \tag{56g}$$

The Roe-type solution (56) is valid for the $x$-split of the two-dimensional shallow water equations (47). For the $z$-sweep one interchanges the roles of the velocity components $u$ and $w$.

It is worth mentioning that the averages (56), in addition to (55), also satisfy

$$\Delta U = U_R - U_R = \sum_{k=1}^{N} \tilde{\alpha}_k \tilde{r}_k, \tag{57}$$

which means that the jump in states across the wave $k$ is given by $\tilde{\alpha}_k \tilde{r}_k$, the product of the wave strength $\tilde{\alpha}_k$ and the appropriate component of the right eigenvector. The same interpretation applies to the flux difference $\Delta F$ in (55). This is split into flux differences across all the waves present in the Riemann problem. The jump in flux across wave $k$ is $\alpha_k \tilde{\lambda}_k \tilde{r}_k$.



PHILOSOPHICAL TRANSACTIONS OF THE ROYAL SOCIETY A MATHEMATICAL, PHYSICAL & ENGINEERING SCIENCES

PHILOSOPHICAL TRANSACTIONS OF THE ROYAL SOCIETY A MATHEMATICAL, PHYSICAL & ENGINEERING SCIENCES

Downloaded from rsta.royalsocietypublishing.org



It should be mentioned here that the Roe's Riemann solver as stated can lead to entropy violating solutions, but entropy fixes can easily be implemented.

Roe's numerical method makes use of (55)–(57). See Glaister (1987) for details.

(vi) *Second interpretation of Roe's solver* (RS2)

The information contained in (56) can be used directly to provide an approximate solution to the Riemann problem in the sense of § 2*a*, namely, an approximation to the star state $U^*$ and the wave speeds.

Equation (57) applied to the two-dimensional equations (47) gives

$$\phi^* - \phi_L = \tilde{\alpha}_1, \quad \phi_R - \phi^* = \tilde{\alpha}_3,$$
$$\phi^* u^* - \phi_L u_L = \tilde{\alpha}_1(\tilde{u} - \tilde{a}), \quad \phi_R u_R - \phi^* u^* = \tilde{\alpha}_3(\tilde{u} + \tilde{a}).$$

It follows that

$$\phi^* = \tfrac{1}{2}(\phi_L + \phi_R + \tilde{\alpha}_1 - \tilde{\alpha}_3), \tag{58}$$

$$u^* = \frac{\phi_L u_L + \phi_R u_R + \tilde{\alpha}_1(\tilde{u} - \tilde{a}) - \tilde{\alpha}_3(\tilde{u} + \tilde{a})}{\phi_L + \phi_R + \tilde{\alpha}_1 - \tilde{\alpha}_3}. \tag{59}$$

One could also obtain values for $w_L^*$ and $w_R^*$ using the Roe averages but this solution would be incorrect. By inspecting (56*f*) and (56*g*) one can see that $w$ changes across the acoustic waves by $\tilde{\alpha}_1 \tilde{w}$ and $\tilde{\alpha}_3 \tilde{w}$ respectively. In the exact solution $w$ only changes across the contact waves. This defect in the Roe approximation can lead to some numerical problems. The same remark applies to the Euler equations in two and three dimensions. The problem becomes apparent in shear waves. I am currently investigating this issue in detail

For a method that is independent of the details of any particular Riemann approximation, such as WAF, one can easily modify the Roe solution for the passive velocity $w$. We simply set $w = w_L$ to the left of the wave $dx/dt = u^*$ and $w = w_R$ otherwise as in the exact solution (49).

For the wave speeds in this interpretation of the Roe solver we take $\lambda_1$, $\lambda_2$ and $\lambda_3$ as given by (52).

(vii) HLL-*type approximations*

Harten *et al.* (1983) suggested some very simple types of approximations to the solution of Riemann problems. We denote this approach by HLL. They begin by considering estimates for bounds on the smallest and largest signal velocities in the solution of the Riemann problem.

Suppose these estimates $E_L$ and $E_R$ say, are available and that $E_L < 0$ and $E_R > 0$ (see figure 6). Consider first the one-dimensional case of equation (5) in the integral form (4). Evaluation of (4) round the rectangle ABCD in figure 6 gives

$$|AO|U_L + |OB|U_R - |CD|U^* - |BC|F_R + |DA|F_L = 0.$$

But the distances are related to the time $|BC| = |DA|$ via the wave speeds $E_L$ and $E_R$ as follows

$$|AO| = -|BC|E_L, |OB| = |BC|E_R.$$

Also
$$|AB| = |CD| = |AO| + |OB| = |BC|(E_R - E_L),$$

from which it follows that

$$|BC|(E_R - E_L)\, U^* = |BC|(E_R\, U_R - E_L\, U_L - F_R + F_L)$$

Downloaded from rsta.royalsocietypublishing.org



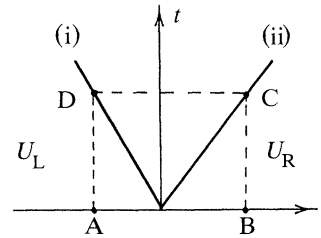


Figure 6. HLL solution of the Riemann problem. $E_L$ and $E_R$ are estimates for the smallest and largest signal velocities. (i) $dx/dt = E_L$; (ii) $dx/dt = E_R$.

and so

$$U^* = (E_R U_R - E_L U_L + F_L - F_R)/(E_R - E_L). \tag{60}$$

One could also compute the star fluxes directly as

$$F^* = (E_R F_L - E_L F_R + E_L E_R (U_R - U_L))/(E_R - E_L). \tag{61}$$

There is freedom in choosing the estimates $E_L$ and $E_R$. Davis (1988) proposed various alternatives. Here we suggest

$$\left.\begin{aligned} E_L &= \lambda_1 = \min\{u_L - a_L, \quad u^*_{TR} - a^*_{TR}\}, \\ E_R &= \lambda_2 = \max\{u_R - a_R, \quad u^*_{TR} + a^*_{TR}\}, \end{aligned}\right\} \tag{62}$$

where $u^*_{TR}$ and $a^*_{TR}$ are the values given by the two-rarefaction approximation (50)–(51).

For the two-dimensional split equations (68) the HLL solver is extended by setting $\lambda_3 = E_R$ in (62) and adding

$$\left.\begin{aligned} &\lambda_2 = u^*, \\ &w(x,t) = \begin{cases} w_L & \text{if} \quad x/t < u^*, \\ w_R & \text{if} \quad x/t > u^*. \end{cases} \end{aligned}\right\} \tag{63}$$

The HLL-type approximation (60) and (62) is very simple and robust. For the shallow water equations this type of approximation is bound to be more successful than for the Euler equations, for which the neglecting of the contact wave leads to excessive smearing of contact surfaces. For the shallow water equations the acknowledgement of only two waves is correct, provided the solution for the passive velocity $w$ is then taken as in (63), for the two-dimensional case.

For fully subcritical ($E_L, E_R \leqslant 0$) and fully supercritical ($E_L, E_R \geqslant 0$) one can still carry out the integration (4). The result is, in either case, a pair of nonlinear algebraic equations for $u^*$ and $\phi^*$. Instead we propose the following procedure: acknowledge a single wave of speed $\lambda$ and take the solution

$$U(x,t) = \begin{cases} U_L, & \text{if} \quad x/t \leqslant \lambda, \\ U_R, & \text{if} \quad x/t > \lambda, \end{cases} \tag{64}$$

with

$$\lambda = \begin{cases} \min\{E_L, E_R\}, & \text{if} \quad E_L, E_R \leqslant 0, \\ \max\{E_L, E_R\}, & \text{if} \quad E_L, E_R \geqslant 0. \end{cases} \tag{65}$$

Note that (64)–(65) could be applied to all conserved variables, as well as the passive velocity.

Downloaded from rsta.royalsocietypublishing.org



Figure 7

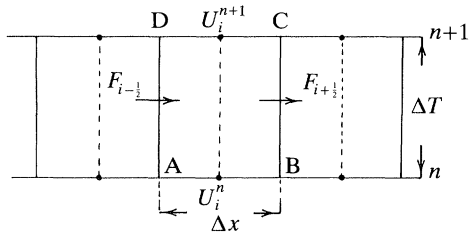


Figure 8

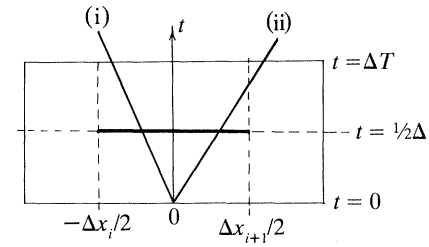


Figure 7. Computational grid in the $xt$-plane. The computing cell $i$ has dimensions $\Delta x$ by $\Delta t$.

Figure 8. Integration path for the WAF-flux evaluation. The illustration is for a $2\times 2$ system such as the one-dimensional shallow water equations. (i) $\mathrm{d}x/\mathrm{d}t = \lambda_1$; (ii) $\mathrm{d}x/\mathrm{d}t = \lambda_2$.

## 3. The weighted average flux method (WAF)

Here we describe a conservative shock capturing method that is applicable to the two-dimensional shallow water equations (1) and uses, locally, the solution of the relevant Riemann problem. We call the method WAF, which stands for weighted average flux. Further details can be found in Toro (1989*a*, *b*, 1990).

The method is directly applicable to hyperbolic conservation laws of the form (4), or (5). Consider a computational grid in the $xt$-plane as shown in figure 7. Application of the integral form of the conservation law (5) to the rectangle ABCD in figure 7 gives the explicit conservative method

$$U_i^{n+1} = U_i^n + (\Delta t/\Delta x)\,[F_{i-\frac{1}{2}} - F_{i+\frac{1}{2}}]. \tag{66}$$

### (*a*) *Formulations of the* WAF *method*

The WAF method uses an intercell flux $F_{i+\frac{1}{2}}$ that is obtained from an integral average of the flux function $F(U)$ across the complete wave structure of the local Riemann problem with piece-wise constant data $(U_i^n, U_{i+1}^n)$. That is to say

$$F_{i+\frac{1}{2}} = \frac{1}{\frac{1}{2}\Delta x_i}\int_{-\frac{1}{2}\Delta x_i}^{0} F(U^*)\,\mathrm{d}x + \frac{1}{\frac{1}{2}\Delta x_{i+1}}\int_{0}^{\frac{1}{2}\Delta x_{i+1}} F(U^*)\,\mathrm{d}x, \tag{67}$$

where $U^* = U^*(x/\frac{1}{2}\Delta t\, U_i^n,\ U_{i+1}^n)$ is the solution of the Riemann problem with data $U_i^n, U_{i+1}^n$ at the half-time level. The Riemann problem is centred at $x = 0$ and its solution depends on the similarity variable $x/t$. In (67) we are allowing for irregular grids; $\Delta x_i$ is the spacing for the computing cell $i$. Figure 8 illustrates the WAF-like evaluation for a $2\times 2$ hyperbolic system, such as the one-dimensional shallow water equations (5).

The integration in (67) could be done exactly, but that would be costly and unnecessary. If we assume that all waves are represented by single rays through the origin, then (67) becomes a summation, namely

$$F_{i+\frac{1}{2}}^{\mathrm{WAF}} = \sum_{k=1}^{N+1} W_k F_{i+\frac{1}{2}}^{(k)}, \tag{68}$$

where, for generality, $N$ represents the number of waves in the Riemann problem. For the one-dimensional shallow water equations $N = 2$. The coefficient $W_k$ in (68) represents the geometric extent of the region $k$ in which the flux function $F(U^*)$ takes

Downloaded from rsta.royalsocietypublishing.org



on the constant value $F^{(k)}_{i+\frac{1}{2}}$. Effectively, $W_k$ is a weight and can be easily seen to be given by

$$W_k = \tfrac{1}{2}(\nu_k - \nu_{k-1}), \quad \nu_0 = -1, \quad \nu_{N+1} = +1. \tag{69}$$

Note that $W_k \geqslant 0$ for all $k$ and $\sum_{k=1}^{N+1} W_k = 1$.

The quantity $\nu_k$ in (69) is the Courant number associated with the wave $k$, of speed $\lambda_k$, in the solution of the local Riemann problem. That is

$$\nu_k = \Delta t\, \lambda_k / \Delta x. \tag{70}$$

The WAF flux is an extension of the Godunov flux, which is defined by

$$F^{\mathrm{GOD}}_{i+\frac{1}{2}} = F[U^*(0, U^n_i, U^n_{i+1})], \tag{71}$$

i.e. $U^*$ is evaluated along the ray $x/t = 0$. Both fluxes use the same Riemann problem, but $F^{\mathrm{GOD}}_{i+\frac{1}{2}}$ gives a first-order accurate method, while $F^{\mathrm{WAF}}_{i+\frac{1}{2}}$ gives a second-order accurate method.

Expansion of formulae (68) and (69) gives a more revealing expression for WAF flux, namely

$$F^{\mathrm{WAF}}_{i+\frac{1}{2}} = \tfrac{1}{2}(F_i + F_{i+1}) - \tfrac{1}{2} \sum_{k=1}^{N} \nu_k \, \Delta F^{(k)}_{i+\frac{1}{2}} \tag{72}$$

with

$$\Delta F^{(k)}_{i+\frac{1}{2}} = F^{(k+1)}_{i+\frac{1}{2}} - F^{(k)}_{i+\frac{1}{2}} \tag{73}$$

representing the flux jump across the wave $k$. Equations (72), (73) reveal the wave splitting character of the intercell flux.

Instead of obtaining an intercell averaged flux one could obtain an averaged state $\bar{V}_{i+\frac{1}{2}}$ as

$$\bar{V}_{i+\frac{1}{2}} = \tfrac{1}{2}(V^n_i + V^n_{i+1}) - \tfrac{1}{2} \sum_{k=1}^{N} \nu_k \, \Delta V^{(k)}_{i+\frac{1}{2}} \tag{74}$$

and then set

$$F_{i+\frac{1}{2}} = F(\bar{V}_{i+\frac{1}{2}}). \tag{75}$$

For linear problems (72) and (75) are identical. For nonlinear problems they formally differ, but numerical results are virtually identical. Formula (75) may, in some cases, be computationally cheaper, but this will depend on the way the Riemann problem solution is made available by the solver. The variable $V$ in (74) can be the conservative variable $U$ or some other convenient choice, such as the primitive variables. If $V$ is the vector of conserved variables then the WAF method is analogous to the Richtymer–Morton, or two-step Lax–Wendroff, method (Richtmyer & Morton 1967).

### (*b*) *Sonic flow problem*

In deriving the approximate expression (72), or (74) and (75), for the WAF intercell flux, it was assumed that the waves in the solution of the Riemann problem were single rays. For contacts and shocks this assumption is correct, but it is not for rarefaction waves, which have a fan-like configuration. This simplification only appears to cause difficulties when the rarefaction fan is centred around the $t$-axis, i.e. when for one of the characteristic rays of the rarefaction wave one has $\mathrm{d}x/\mathrm{d}t = u - a = 0$ (for a left rarefaction) or $\mathrm{d}x/\mathrm{d}t = u + a = 0$ (for a right rarefaction). In such circumstances one speaks of locally sonic flow.

The two possible cases for the one-dimensional shallow water equations are illustrated in figure 9.

Downloaded from rsta.royalsocietypublishing.org



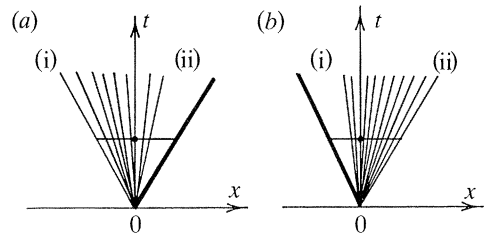


Figure 9. Locally sonic flow. Case (*a*) shows the solution of a Riemann problem where the left wave is a rarefaction centred around the $t$-axis, i.e. $u = a$ along the $t$ axis. (i) $\mathrm{d}x/\mathrm{d}t = u_{\mathrm{L}} - a_{\mathrm{L}} < 0$; (ii) $\mathrm{d}x/\mathrm{d}t = u^* - a^* > 0$. Case (*b*) illustrates the sonic-flow situation for a right rarefaction. (i) $\mathrm{d}x/\mathrm{d}t = u^* + a^* < 0$; (ii) $\mathrm{d}x/\mathrm{d}t = u_{\mathrm{R}} + a_{\mathrm{R}} > 0$.

Locally sonic flow is related to the property of entropy satisfaction for conservative schemes. See Harten *et al.* (1983) for details. Entropy violating schemes can compute 'rarefaction shocks', which are unphysical. The WAF method with the exact Riemann solver is entropy satisfying provided one replaces the $U^*$ constant state between the acoustic waves by the point value $U^*(0, U_i, U_{i+1})$, which is the value at which the Godunov flux is evaluated. For the shallow water equations the exact solution at $x/t = 0$ is given by equations (43)–(46).

In general, it is the Riemann-problem solution that plays the crucial role. Certain approximations, such as the Roe approximation (56), are known to be entropy violating. Special entropy fixes are then required.

The inherent second-order accuracy of the WAF method leads to spurious oscillations near shock waves or other discontinuities. The local wave structure of the Riemann problem can be used to construct an oscillation free version of the method.

### (*c*) *A* TVD *version of* WAF

Given the discrete solution $\{U_i^n\}$ at time level $n$ the total variation of $\{U_i^n\}$ is defined as

$$TV(U^n) = \sum_i |U_{i+1}^n - U_i^n|.$$

This is essentially a measure of the oscillatory character of the solution. Many useful difference schemes are total variation diminishing, or TVD for short. That is the total variation diminishes with time, or

$$TV(U^{n+1}) \leqslant TV(U^n).$$

For the model linear advection equation

$$U_t + aU_x = 0$$

we can construct rigorously a TVD version of WAF. See Toro (1989*e*) for details. For nonlinear systems the TVD procedure is empirical, but in practice it works very well as will be demonstrated in §4.

The principle is to amplify the wave speeds in the solution of the local Riemann problem. The purpose is to alter the size of the weights $W_k$ while keeping the states unaltered. This is achieved by multiplying the Courant numbers $\nu_k$ by an amplifying function $A_k$. Thus the oscillation-free WAF flux (72) becomes

$$F_{i+\frac{1}{2}} = \tfrac{1}{2}(F_i + F_{i+1}) - \tfrac{1}{2} \sum_{k=1}^{N} A_k \nu_k \Delta F_{i+\frac{1}{2}}^{(k)}. \tag{76}$$

Downloaded from rsta.royalsocietypublishing.org



The amplifying function $A_k = A_k(U)$ is a function of the flow features. Here we give one such function

$$A_k = \begin{cases} (1-2(1-|\nu_k|))/|\nu_k|, & r_i \geqslant 2, \\ (1-r_i(1-|\nu_k|))/|\nu_k|, & 1 \leqslant r_i \leqslant 2, \\ 1, & \frac{1}{2} \leqslant r_i \leqslant 1, \\ (1-2r_i(1-|\nu_k|))/|\nu_k|, & 0 \leqslant r_i \leqslant \frac{1}{2}, \\ 1/|\nu_k|, & r_i \leqslant 0. \end{cases} \tag{77}$$

The definition (77) for $A_k$ is for a single wave $k$ with Courant number $\nu_k$. We call $A_k$ SUPERA, in analogy with the flux limiter SUPERB. The flow parameter $r_i$ is

$$r_i = \begin{cases} \Delta Q^{(k)}_{i-\frac{1}{2}}/\Delta Q^{(k)}_{i+\frac{1}{2}} & \text{if} \quad \nu_k \geqslant 0, \\ \Delta Q^{(k)}_{i+\frac{3}{2}}/\Delta Q^{(k)}_{i+\frac{1}{2}} & \text{if} \quad \nu_k < 0, \end{cases} \tag{78}$$

where $Q$ is a suitable variable. For the shallow water equations we use $Q = \phi$ for the acoustic waves and $Q = w$ for the 'contact' wave. The notation $\Delta Q^{(k)}_{i+\frac{1}{2}}$ mean the jump in $Q$ across the wave $k$ in the Riemann problem with data $(U_i, U_{i+1})$. The denominator in (78) is always the jump through wave $k$ in the local Riemann problem $(i, i+1)$, whereas the numerator looks at the upstream or upwind direction to find the appropriate jump. Since the waves in the Riemann problem generally travel in different directions one must construct a function $A_k$ for each wave $k$.

If the version (74)–(75) of WAF is to be used then the oscillation-free average state $\bar{V}_{i+\frac{1}{2}}$ is given by

$$\bar{V}_{i+\frac{1}{2}} = \tfrac{1}{2}(V^n_i + V^n_{i+1}) - \tfrac{1}{2}\sum_{k=1}^{N} A_k \nu_k \Delta V^{(k)}_{i+\frac{1}{2}}. \tag{79}$$

### (*d*) *The* CFL *condition*

The WAF method (66) with (76), or (79), is an explicit time-marching scheme. The stable rate of advance in time is given by the Courant condition. Here we suggest a nonlinear CFL condition as proposed in Toro (1989*d*).

For a given cell $i$ there is a time step $\Delta t_i$ that is the time it takes for the right acoustic wave of speed $S^{\mathrm{R}}_{i-\frac{1}{2}}$ from the left Riemann problem $(i-1, i)$ to intersect the left acoustic wave of speed $S^{\mathrm{L}}_{i+\frac{1}{2}}$ of the right Riemann problem $(i, i+1)$. If the size of the cell $i$ is given by $\Delta x_i$, then

$$\Delta t_i = \Delta x_i/(S^{\mathrm{L}}_{i+\frac{1}{2}} - S^{\mathrm{R}}_{i-\frac{1}{2}}). \tag{80}$$

Then we take $\Delta t$, the time-step size for the scheme at the given time level, as $\Delta t = \min\{\Delta t_i\}$. Due to the denominator in (80), it is best for programming purposes to take

$$\left.\begin{aligned} \Delta t &= \Delta x/S_{\max}, \\ S_{\max} &= \max_i \{S^{\mathrm{L}}_{i+\frac{1}{2}} - S^{\mathrm{R}}_{i-\frac{1}{2}}\}. \end{aligned}\right\} \tag{81}$$

A simpler, but less reliable CFL condition is

$$\Delta t = \min_i \{\Delta x_i/2a^n_i\}, \tag{82}$$

where $a^n_i$ is the sound speed at $i$ at the data time level. This is a special case of

Downloaded from rsta.royalsocietypublishing.org



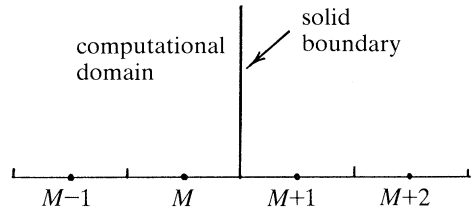


Figure 10. Right-hand boundary. Two fictitious states $M+1$ and $M+2$ are required.

(80)–(81) with $S^{\mathrm{L}}_{i+\frac{1}{2}} = u^n_i - a^n_i, S^{\mathrm{R}}_{i-\frac{1}{2}} = u^n_i + a^n_i$. Both (81) and (82) are better than the commonly used empirical formula $\Delta t = C\Delta x/S$, where $S$ is the maximum wave speed present in the data, usually taken as $S = \max_i\{|u^n_i| + a^n_i\}$. $C$ is an empirical coefficient with $0 < C \leqslant 1$. For shock-tube like initial data ($u^n_i \equiv 0$) this condition fails and can lead to serious stability problems at the beginning of the calculations.

### (e) *Boundary conditions*

We describe two types of boundary conditions that are applicable to one-dimensional problems.

#### (i) *Reflective boundaries*

If the presence of solid walls, fixed or moving, reflective boundary conditions must be imposed. Consider the boundary on the right-hand side of the computational domain, as shown in figure 10. The last two cells inside the computational domain are $M-1$ and $M$. Two fictitious computational cells are added to the right-hand side of the solid boundary; these are denoted by $M+1$ and $M+2$. For simplicity consider the Riemann problem $RP(M, M+1)$. The correct Riemann problem is the one whose solution has $u^* = v_{\mathrm{B}}$ = velocity of the solid boundary. It can be easily verified that for this to happen the fictitious state $M+1$ must be given by

$$\phi_{M+1} = \phi_M, \quad u_{M+1} = -u_M + 2v_{\mathrm{B}}. \tag{83a}$$

To preserve second-order accuracy we also need

$$\phi_{M+2} = \phi_{M-1}, \quad u_{M+2} = -u_{M-1} + 2v_{\mathrm{B}}. \tag{83b}$$

#### (ii) *Transmissive boundaries*

There are cases in which one is only interested in the local behaviour of the solution, or one may wish to simulate a boundary at infinity or a transmissive boundary. This can be achieved by placing 'transparent' boundaries that allow waves to pass through.

With reference to figure 10 one imposes

$$\left.\begin{aligned} \phi_{M+1} = \phi_M, \quad u_{M+1} = u_M, \\ \phi_{M+2} = \phi_{M-1}, \quad u_{M+2} = u_{M-1}. \end{aligned}\right\} \tag{84}$$

Note that the solution of the Riemann problem $RP(M, M+1)$ is trivial. It is important to realize that the boundary condition (84) does not impose zero gradient of the solution at the boundary, which would be incorrect. But care is required with this artificial boundary condition, for small spurious reflections may be caused.

Downloaded from rsta.royalsocietypublishing.org



### (*f*) *Extensions of the method*

We describe two extensions of the WAF method so that the full two-dimensional problem with source terms

$$U_t + F_x + G_z = S(U) \tag{85}$$

can be solved.

(i) *Treatment of source terms*

Consider the one-dimensional inhomogeneous problem

$$U_t + F_x = S(U). \tag{86}$$

The source term $S(U)$ can include $[0, g\phi h_x]^{\mathrm{T}}$ as well as some other effects such as Coriolis forces and bottom roughness.

We use time-operator splitting so that the problem (86) with initial data $U^n$ is split into two sub-problems. One proceeds as follows:

(*a*) Solve the homogeneous problem

$$U_t + F_x = 0$$

with data $U^n$ to obtain a provisional solution $\bar{U}^{n+1}$ for the next time level.

(*b*) Solve the system of ordinary differential equations (ODEs)

$$U_t = S(U)$$

by using as initial condition the provisional solution $\bar{U}^{n+1}$ of the previous step. This gives the final solution $U^{n+1}$ for the new time level $n+1$.

The choice of the numerical method for solving the ODEs depends very much on the character of the sources. For most problems a Runge–Kutta method is good enough, although the simpler first-order Euler step

$$U_i^{n+1} = \bar{U}_i^{n+1} + \Delta t S(\bar{U}_i^{n+1})$$

is used very frequently. Here $\Delta t$ is the time-step size given by the CFL condition in the homogeneous step (1). If the ODEs are a stiff system an implicit method must be used.

The terms involving derivatives, such as $h_x$ can be approximated using central differences, say. If $h(x)$ is known at the intercell boundaries then a second-order approximation at the cell centre would be $h_x \approx (h_{i+\frac{1}{2}} - h_{i-\frac{1}{2}})/\Delta x$.

(ii) *Treatment of a second dimension*

Consider the two-dimensional problem

$$U_t + F_x + G_y = 0$$

with data $U^n$. We use space-operator splitting whereby the problem is solved in two sweeps.

*x-sweep*: solve

$$U_t + F_x = 0$$

with data $U^n$ to obtain a provisional solution $U^{n+\frac{1}{2}}$.

Note that this problem is an extended one-dimensional problem. See equation (1). There is a third equation involving the 'passive' component of velocity $w$. The extended Riemann-problem solution must be used.

Downloaded from rsta.royalsocietypublishing.org



*z-sweep*: solve

$$U_t + G_z = 0$$

with initial data $U^{n+\frac{1}{2}}$. The solution of this step is the final solution $U^{n+1}$ for the time level $n+1$. The time step size $\Delta t$ is chosen at the beginning of the splitting procedure and it is common to both the $x$ and $z$ sweeps. If sources were present one would require another step, as described previously.

There are more sophisticated combinations of the $x$ and $z$ sweeps that would ensure formal second-order accuracy. See Strang (1968) for details.

### (g) *An algorithm for the one-dimensional case*

We summarize the main steps involved in the implementation of WAF as applied to the homogeneous one-dimensional shallow water equations (5). Having specified the domain length, the number of computing cells $M$ and the grid size $\Delta x$ the following operations are performed at every time step $n$:

(*a*) Solve the Riemann problem $RP(i, i+1)$ and store (i) the wave speeds into $WS(1, i)$, $WS(2, i)$; (ii) the $\phi$-jumps across each wave into $WJ(1, i)$, $WJ(2, i)$; (iii) the flux values in the star region into $FS(1, i)$, $FS(2, i)$.

The fluxes may have to be computed from the star values $\phi^*, u^*$ or they may be directly available from the solution of the Riemann problem, as when using the HLL approximation given by equation (61), for instance.

Here the loop runs from $i = -1$ to $M+1$.

(*b*) Apply the CFL condition (81) to find $\Delta t$.

(*c*) For each $i$, $i = 0$ to $M$: (i) compute the local Courant numbers $\nu_k = WS(k, i)\,\Delta t/\Delta x$, $k = 1, 2$; (ii) compute the amplifiers $A_k$ (using equation (77), say), $k = 1, 2$; (iii) modify Courant numbers, $\nu_k = A_k \nu_k$; (iv) compute the intercell fluxes according to (76), say. Store values into $FI(1, i)$, $FI(2, i)$.

(*d*) Advance to the next time level $n+1$ using the conservative formula (66).

## 4. Test problems

Three test problems are used to assess the performance of the WAF method using the various Riemann solvers described in §3. Test problems 1 and 2 are one-dimensional cases: for which the first one has known exact solution; the second one involves a source term due to a non-horizontal bed. Test problem 3 is a two-dimensional time-dependent problem, whose exact solution is unknown to us. There are, however, certain features of the solution which can be used to judge the numerical results.

### (a) *Test 1*

A one-dimensional domain of length 1.0 is chosen. We take $M = 100$ so that $\Delta x = 0.01$. The initial data is that for a dam-break problem

$$\phi(x, 0) = \begin{cases} \phi_{\mathrm{L}} = 1.0, & 0 \leqslant x \leqslant \frac{1}{2}, \\ \phi_{\mathrm{R}} = 0.1, & \frac{1}{2} < x \leqslant 1.0, \end{cases}$$

and $u(x, 0) = 0$ for all $x$ in $[0, 1]$. The CFL condition is that given by equation (81). This nonlinear CFL condition gives the maximum time-step size without wave interaction within a cell.

The computed solution is evolved to time $t = 0.4$ units. Figure 11 shows the exact solution in full line for the flow variable $\phi(x, t)$ and the particle speed $u(x, t)$ together

Downloaded from rsta.royalsocietypublishing.org



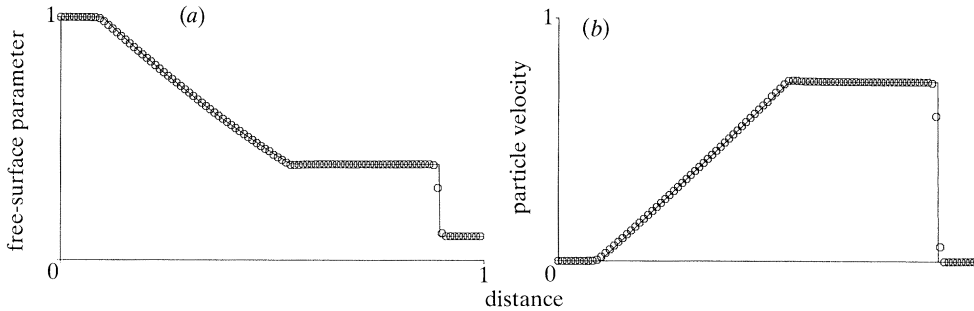


Figure 11. Numerical (symbol) and exact (line) solutions to test 1 at time $t = 0.4$ units. The WAF method with the exact Riemann solver and the TVD function SUPERA is used to compute the numerical solution.

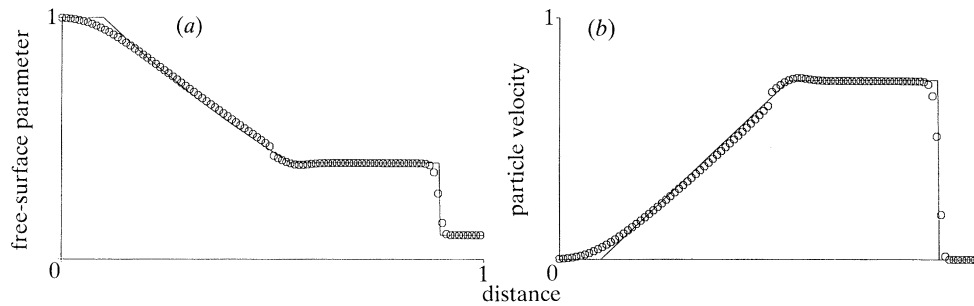


Figure 12. Numerical (symbol) and exact (line) solutions to test 1 at time $t = 0.4$ units. The Godunov method with the exact Riemann solver is used to compute the numerical solution.

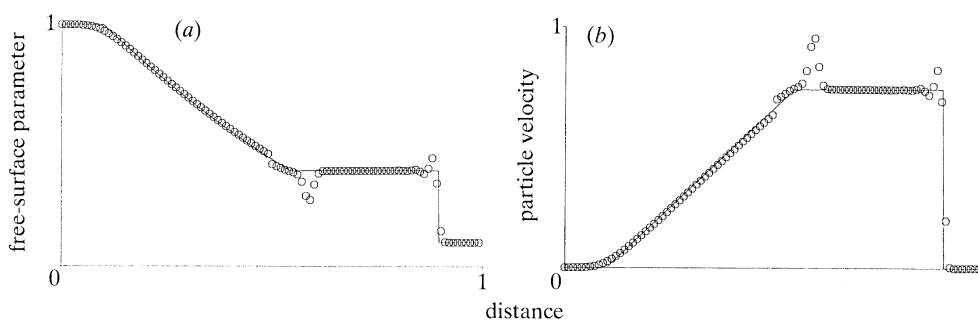


Figure 13. Numerical (symbol) and exact (line) solutions to test 1 at time $t = 0.4$ units. The Richtmyer–Morton version of WAF with the exact Riemann solver is used to compute the numerical solution.

with the numerical solution, shown in symbols. These results were obtained by the WAF method with the exact Riemann solver and the amplifier SUPERA of equation (77).

The numerical results of figure 12 were obtained by using the first-order Godunov's method together with the exact Riemann solver. The shock wave is reasonably well resolved by four to five grid points. There are no oscillations behind the shock. The rarefaction wave, however, is very poorly represented. The excessive numerical diffusion inherent in this first-order accurate method is clearly manifested near 'corners', where the solution has a discontinuity in derivative. Also the entropy problem of Godunov's method can be seen around $x = \frac{1}{2}$ in figure 12. This method is

Downloaded from rsta.royalsocietypublishing.org



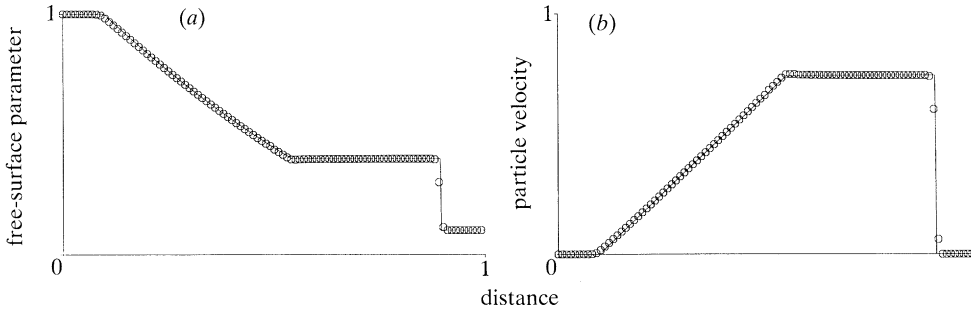


Figure 14. Numerical (symbol) and exact (line) solutions to test 1 at time $t = 0.4$ units. The WAF method with the TS-approximate Riemann solver and the TVD function SUPERA is used to compute the numerical solution.

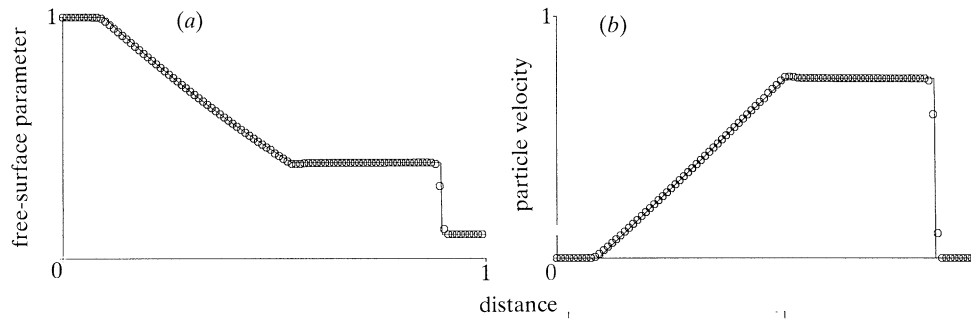


Figure 15. Numerical (symbol) and exact (line) solutions to test 1 at time $t = 0.4$ units. The WAF method with the TR-approximate Riemann solver and the TVD function SUPERA is used to compute the numerical solution.

theoretically entropy satisfying and thus the entropy glitch should vanish as the mesh size vanishes. For finite grids, however, the glitch is visible although it is not a serious problem.

Figure 13 shows the results obtained by the fully second-order method with $A_k = 1$. The accuracy in smooth parts of the flow is now better. Also, the discontinuities are more sharply resolved, including the head and the tail of the rarefaction. The entropy glitch is worse than that of Godunov's method, as expected. The most serious problem, however, is that of the spurious oscillations. The overall solution is unacceptable.

Figures 14 to 16 show results using the WAF method with approximate Riemann solvers; they are the two-shock (TS), the two-rarefaction (TR) and the Roe-type solver (RS2) respectively. These results are very good. The quality of the solution is preserved even if approximate Riemann solvers are used. For this test problem the results obtained by using the approximate Riemann solvers are, to plotting accuracy, almost indistinguishable from those of the exact Riemann solver.

### (b) *Test 2*

This test involves a one-dimensional channel 30 m long whose non-uniform bed elevation $b(x)$ (above a horizontal datum) is given by:

$$b(x) = 0 \quad \text{if} \quad x\epsilon[0, 10],$$

$$b(x) = 1.0 \quad \text{if} \quad x\epsilon[20, 30],$$

Downloaded from rsta.royalsocietypublishing.org



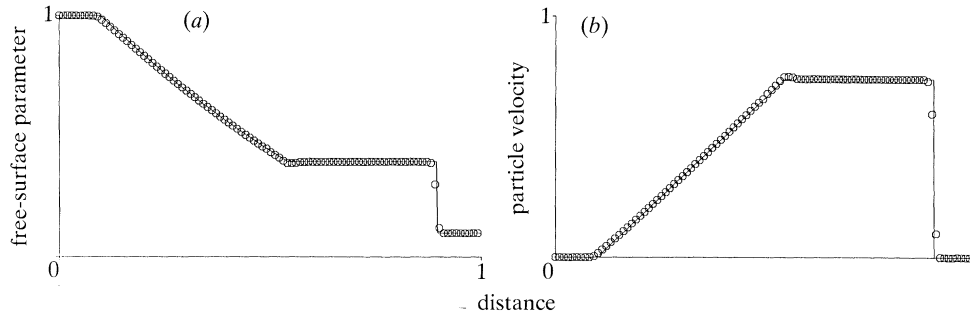


Figure 16. Numerical (symbol) and exact (line) solutions to test 1 at time $t = 0.4$ units. The WAF method with the RS2-approximate Riemann solver and the TVD function SUPERA is used to compute the numerical solution.

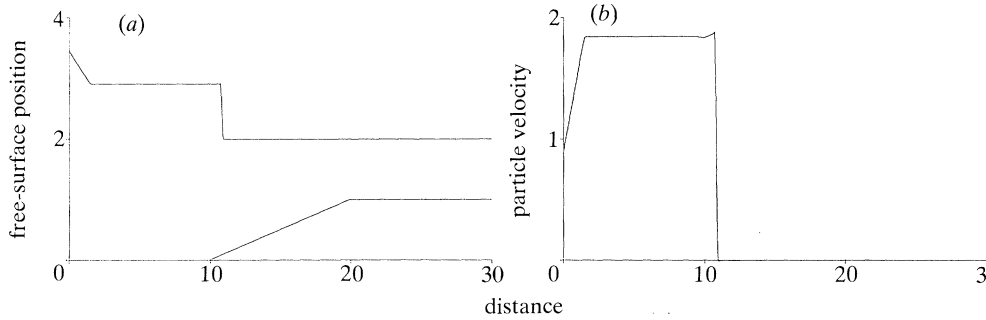


Figure 17. Numerical solution of Test 2 for the free surface $h+\eta$ and $u$ at time $t = 1$ s. The exact Riemann solver and SUPERA are used.

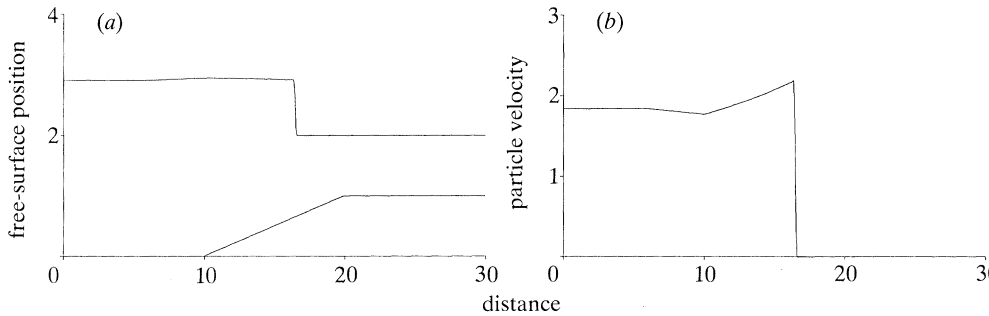


Figure 18. Numerical solution of Test 2 for $h+\eta$ and $u$ at time $t = 2$ s.

and $b(x)$ varies linearly between 0 and 1 m for $x\epsilon[10, 20]$. The resulting source term is treated by the time-operator splitting method described in §3*f*.

The initial conditions are

$$H(x,0) = \begin{cases} H_{\mathrm{L}} = 4 \text{ m}, & x\epsilon[0,5], \\ H_{\mathrm{R}} = 2 \text{ m}, & x\epsilon[5,30], \end{cases}$$

where $H$ denotes the total elevation of the free surface.

Figures 17 to 19 show the computed results at times 1 s, 2 s and 4 s respectively. The computations were performed on a grid of 400 cells.

The exact Riemann solver was applied. Figure 17 shows the right travelling bore

Downloaded from rsta.royalsocietypublishing.org



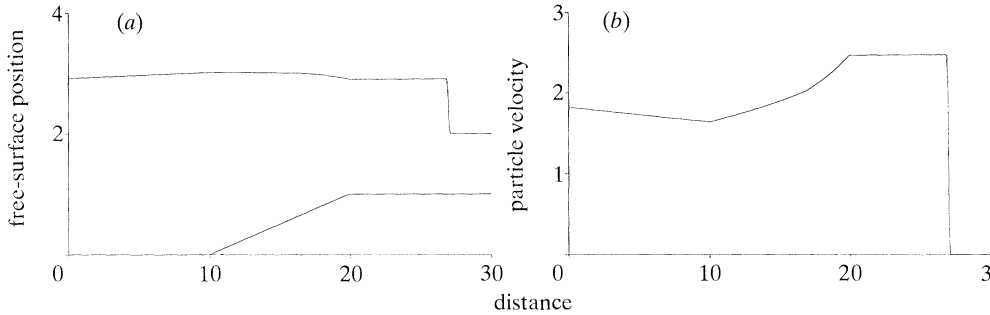


Figure 19. Numerical solution of Test 2 for $h+\eta$ and $u$ at time $t = 4$ s.

and the left depression that emerge from the break up of the initial discontinuity. The boundary conditions on the left boundary are transmissive and thus the rarefaction travels outside the computational domain. At the time shown the bore has just passed the beginning of the bed elevation, the effect of which is seen mainly in the particle velocity profile. Figure 18 shows, at $t = 2$ s, an appreciable effect of the bed elevation on the particle velocity distribution. The free surface position is also affected, as expected. Figure 19 shows the solution at $t = 4$ s. Both the free surface position and the particle velocity have recovered a distribution expected on a horizontal bed.

### (c) *Test 3*

This is a two-dimensional problem that simulates the collapse of a circular dam. The computational domain is $[0,2]x[0,2]$ in the $xz$-horizontal plane. The dam is centred at $(1,1)$ and its radius is 0.35. The initial conditions are $u(x,z,0) = w(x,z,0) = 0$ and

$$\phi(x,z,0) = \begin{cases} 1.0 & \text{if} \quad (x-1)^2+(z-1)^2 \leqslant (0.35)^2, \\ 0.1 & \text{otherwise.} \end{cases}$$

Figures 20 and 21 show the computed solution for $\phi(x,z,t)$ at times $t = 0.2$ and $t = 0.46$ units respectively.

The leading circular bore is attenuated as time evolves as one would expect. The mechanism that makes that possible is the depression wave overtaking the bore, i.e. $\phi$ decreases from the bore towards the centre up to the tail of the depression wave running into the centre $(1,1)$. These numerical results were obtained by using WAF with the TR approximation.

## 5. Conclusions

Several Riemann solvers for the shallow-water equations have been presented. These have been used locally in the weighted average flux method (WAF) to compute the global solution to the general initial-boundary value problem for the unsteady, two-dimensional shallow water equations. The algorithms are conservative and have the ability to capture discontinuities with high resolution without the spurious oscillations of traditional higher-order finite difference methods. This is illustrated by the preliminary numerical results presented. The results so far suggest that for applications in which the solution exhibits high gradients and nonlinear effects are important the WAF approach presented here can provide very accurate numerical solutions.



PHILOSOPHICAL TRANSACTIONS OF THE ROYAL SOCIETY A MATHEMATICAL, PHYSICAL & ENGINEERING SCIENCES

PHILOSOPHICAL TRANSACTIONS OF THE ROYAL SOCIETY A MATHEMATICAL, PHYSICAL & ENGINEERING SCIENCES

Downloaded from rsta.royalsocietypublishing.org



Figure 20

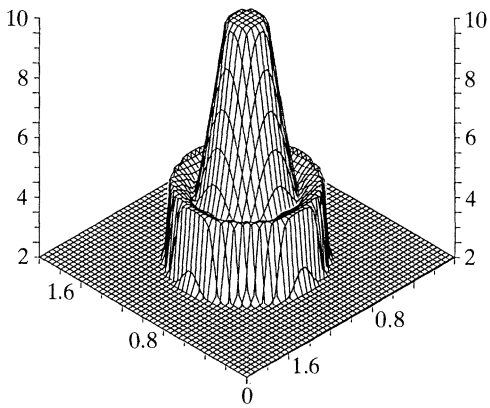


Figure 21

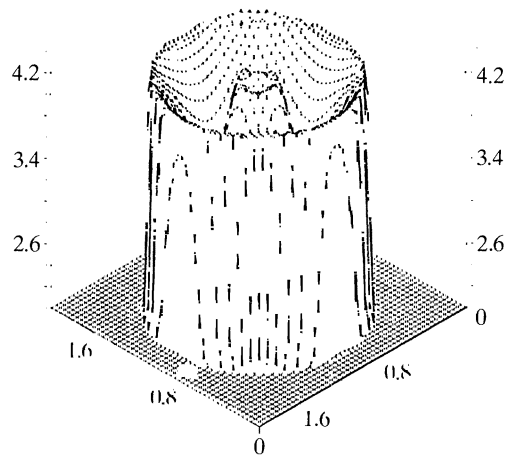


Figure 20. Numerical solution for $\phi$ to Test 3 at time $t = 0.2$ units. The WAF method with the TR-approximate Riemann solver and the TVD function SUPERA is used to compute the numerical solution.

Figure 21. Numerical solution for $\phi$ to Test 3 at time $t = 0.46$ units. The WAF method with the TR-approximate Riemann solver and the TVD function SUPERA is used to compute the numerical solution.

A significant part of this work was carried out at the Mathematics Department, University of Trento, Italy, while the author was visiting Trento at the kind invitation of Professor Vincenzo Casulli. The support provided is gratefully acknowledged.

## References

Casulli, V. 1990 Numerical simulation of shallow water flow. In *Proc. VIII Conference on Computational Methods in Water Resources, Venice, Italy, June 1990*.

Davis, S. F. 1988 Simplified second-order Godunov-type methods. *SIAM J. Sci. statist. Comput.* **9**, 445–473.

Glaister, P. 1987 Difference schemes for the shallow water equations. Numerical analysis report 9/87. Department of Mathematics, University of Reading, U.K.

Harten, A., Lax, P. D. & van Leer, B. 1983 On upstream differencing and Godunov-type schemes for hyperbolic conservation laws. *SIAM Rev.* **25**, 35–61.

Jeffrey, A. 1976 *Quasilinear hyperbolic systems and waves. Research notes in mathematics*. Pitman.

Marshall, E. & Méndez, R. 1981 Computational aspects of the random choice method for shallow water equations. *J. Comput. Phys.* **39**, 1–21.

Osher, S. & Solomon, F. 1982 Upwind difference schemes for hyperbolic systems of conservation laws. *Math. Comput.* **38**, 339–374.

Richtmyer, R. D. & Morton, K. W. 1967 *Difference methods for initial-value problems*. Wiley-Interscience.

Roe, P. L. 1981 Approximate Riemann solvers, parameter vectors, and difference schemes. *J. Comput. Phys.* **43**, 357–372.

Stoker, J. J. 1957 *Water waves*. New York: Interscience.

Strang, G. 1968 On the construction and comparison of finite difference schemes. *SIAM J. numer. Analysis* **5**, 506–517.

Toro, E. F. 1989*a* A weighted average flux method for hyperbolic conservation laws. *Proc. R. Soc. Lond.* A **423**, 401–418.

Downloaded from rsta.royalsocietypublishing.org



Toro, E. F. 1989*b* Riemann-problem methods for computing reactive two-phase flows. Lecture Notes in Physics vol. 351, pp. 472–481. *Numerical Combustion, Proc. Juan Les Pins, Antibes, France, 1989.*

Toro, E. F. 1989*c* A fast Riemann solver with constant covolume applied to the random choice method. *Int. J. numer. Meth. Fluids* **9**, 1145–1164.

Toro, E. F. 1989*d* A CFL condition for characteristic based methods. *Appl. Math. Lett.* **2**, 57–60.

Toro, E. F. 1989*e* TVD regions for the weighted averaged flux (WAF) method as applied to a model hyperbolic conservation law. CoA report 8907, June 1989, Cranfield Institute of Technology, U.K.

Toro, E. F. 1990 Numerical solution of the Euler equations by the weighted average flux method. CoA report 9001, March 1990, Cranfield Institute of Technology, U.K.

*Received 18 December 1990; revised 11 April 1991; accepted 9 May 1991*



PHILOSOPHICAL TRANSACTIONS OF THE ROYAL SOCIETY A MATHEMATICAL, PHYSICAL & ENGINEERING SCIENCES

PHILOSOPHICAL TRANSACTIONS OF THE ROYAL SOCIETY A MATHEMATICAL, PHYSICAL & ENGINEERING SCIENCES